RSC Advances

ROYAL SOCIETY OF CHEMISTRY

www.rsc.org/advances

Graphical abstract

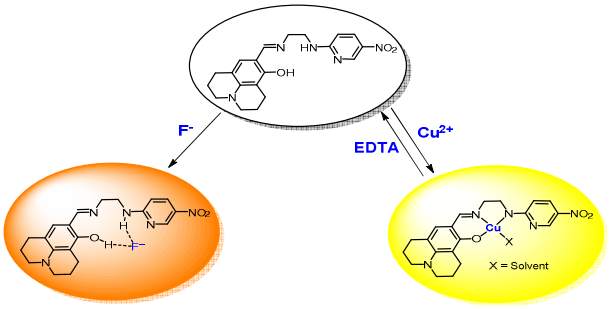

Colorimetric chemosensor was reported for detection of Cu^{2+} and F^- via the color change from colorless to yellow and to orange.

Chromogenic naked-eye detection of copper ion and fluoride

Ye Won Choi, Jae Jun Lee, Ga Rim You, Sun Young Lee, Cheal Kim*

Department of Fine Chemistry and Department of Interdisciplinary Bio IT Materials, Seoul National University of Science and Technology, Seoul 139-743, Korea. Fax: +82-2-973-9149; Tel: +82-2-970-6693; E-mail: chealkim@seoultech.ac.kr

Abstract

A bi-functional colorimetric chemosensor **1**, based on julolidine moiety and *N*-(2-aminoethyl)-5-nitropyridin-2-amine, has been synthesized and characterized. The sensor **1** has proven to be highly selective and sensitive to Cu^{2+} with a color change from colorless to yellow in aqueous solution. The sensing mechanism of **1** for Cu^{2+} was proposed to be the ligand-to-metal charge-transfer (LMCT), which was explained by theoretical calculations. It was also found that the **1**-Cu^{2+} complex could be recycled simply through treatment with an appropriate reagent such as EDTA. Importantly, the sensor **1** could be used to detect and quantify Cu^{2+} in water samples. Moreover, **1** showed a selective colorimetric response toward fluoride due to the increase in the intramolecular charge transfer (ICT) band by a deprotonation process without any inhibition from other anions such as CH_3COO^- and CN^-.

Keywords: chemosensor, copper ion, fluoride, colorimetric, LMCT, ICT

Introduction

Design and synthesis of new chemosensors for transition metal ions and anions have been of interest to chemists for many years because these ions play important roles in the fields of biological, environmental and chemical systems.[1] Among transition metal ions, copper is the third-most abundant transition metal in human, and it plays an important role as a redox catalyst in biological processes such as electron transfer reactions involving oxidation of various organic substrates.[2] However, an excess amount of copper in the body would cause gastrointestinal disturbance, damage to the liver and kidney, Alzheimer's disease, Wilson's disease and Parkinson's disease.[3] The maximum permissible levels of Cu^{2+} in drinking water by World Health Organization (WHO) is 2.0 ppm (31.5 μM).[4] Therefore, it is important to design and develop Cu(II) sensors with high selectivity and sensitivity.

Among various important anionic analytes, fluoride (F^-) is of particular interest owing to its established role in dental care and clinical treatment for osteoporosis.[5] However, an acute intake of a large dose or chronic ingestion of lower doses of fluoride can cause many serious disease such as gastric and kidney disorders, dental and skeletal fluorosis, and urolithiasis in humans, and even death.[6] Also, they contribute significantly to environmental pollution.[7] For these reasons, the improved chemosensor for the detection and sensing of F^- with high selectivity is of current interest. However, many anion sensors are not capable of distinguishing fluoride effectively from anions such as CH_3COO^- and CN^-, because they possess similar basicity to F^- and easily form hydrogen bonds.[8] Therefore, it is highly desirable to develop selective methods capable of discriminating fluoride, especially from competing anions (CH_3COO^- and CN^-).

Up to now, various methods for detecting cations and anions have been developed in a variety of complex environments, such as chromatographic, fluorometric and colorimetric chemosensor, flow injection and electrochemical analysis.[9] Among them, colorimetric chemosensors are the most promising in sensor field as it does not need any expensive instrumentation.[10] The analyte determination can be carried out by the naked eye under visible light. Therefore, it is of considerable importance to develop probes with colorimetric sensing ability for detection of both Cu^{2+} and F^-.

Julolidine moiety has been well known as a chromophore and chemosensors with the julolidine moiety often showed a good colorimetric response with target analytes.[11] On the other hand, the presence of the electron-withdrawing nitro group on the amino-pyridyl moiety would increase not only the degree of π-conjugation but also the hydrogen bonding ability of the amino NH proton.[12] Therefore, we designed and synthesized a new chemosensor **1** based on the combination of the julolidine and nitropyridine moieties, and tested its sensing properties towards various metal ions and anions.

Herein, we report a new bi-functional chemosensor **1** for Cu^{2+} and F^-, which was synthesized in one step by condensation reaction of 8-hydroxyl-julolidine-9-carboxaldehyde and *N*-(2-aminoethyl)-5-nitropyridin-2-amine (Scheme 1). The sensor **1** can detect Cu^{2+} by color change from colorless to yellow in aqueous solution. Additionally, **1** showed a distinctly red-shifted absorption spectrum with the intense color change in the presence of F^-.

Results and discussion

Synthesis of receptor 1

Receptor **1** was obtained by the combination of 8-hydroxyjulolidine-9-carboxaldehyde and *N*-(2-aminoethyl)-5-nitropyridine-2-amine with 84 % yield in ethanol (Scheme 1), and characterized by ^{1}H NMR and ^{13}C NMR, ESI-mass spectroscopy, and elemental analysis.

Colorimetric signaling of 1 to Cu^{2+}

To verify the selectivity, the absorptive behavior of **1** was investigated upon the addition of various metal ions in acetonitrile/buffer solution (7:3; v/v, 10 mM bis-tris, pH 7.0). As shown in Fig. 1, the absorption spectrum of free **1** showed a maximum peak centered at 382 nm. The addition of 12 equiv of Cu^{2+} into the **1** solution resulted immediately in a significant enhancement of absorbance at 450 nm with the color change from colorless to yellow (Fig. 1b). Under the identical condition, there were no appreciable changes of the absorption in the presence of Al^{3+}, Zn^{2+}, Cd^{2+}, Mg^{2+}, Cr^{3+}, Co^{2+}, Ni^{2+}, Na^+, K^+, Ca^{2+}, Mn^{2+}, Pb^{2+}, Fe^{2+} and Fe^{3+}. Hg^{2+}, Ag^+, and Au^{3+} produced precipitate due to their insolubility in acetonitrile/buffer solution (7:3). The results demonstrated that **1** was characteristic of high selectivity toward Cu^{2+} over

other metal ions.

An UV-vis titration experiment was performed to investigate the interaction of Cu^{2+} and **1** (Fig. 2). Upon the gradual addition of Cu^{2+} to a solution of **1**, the absorbance peak at 382 nm steadily decreased and two new absorption bands at 275 and 450 nm appeared concomitantly, resulting in a color change from colorless to yellow. The isosbestic point at 350 nm was clearly observed, indicating the formation of a single species between **1** and Cu^{2+}. Moreover, the new peak at 450 nm in the visible region with molar extinction coefficient in the thousands, 7.32×10^3 M^{-1} cm^{-1}, is too large to be Cu-based d-d transitions and thus must be ligand-based transitions.[13] Therefore, we proposed that the new peak at 450 nm might be attributed to a ligand-to-metal charge-transfer (LMCT).

A Job plot analysis showed a 1:1 stoichiometry for the **1**-Cu^{2+} complex (Fig. S1), which was further confirmed by ESI-mass spectrometry analysis (Fig. S2). The positive ion mass spectrum of ESI-mass indicated that a peak at m/z = 520.73 was assignable to [**1**(-H^+) + Cu^{2+} + DMSO]$^+$ [cald, m/z = 521.12]. Based on Job plot, ESI-mass spectrometry and the crystal structures of similar type of Cu complexes reported in the literature,[14] we proposed the structure of 1:1 complex of **1** and Cu^{2+} as shown in Scheme 1.

From UV-vis titration data, the association constant for **1**-Cu^{2+} complex was determined to be 1.5×10^3 M^{-1} using Benesi-Hildebrand equation[15] (Fig. S3). This value was within the range of those (10^3 - 10^{12}) reported for Cu^{2+} sensing chemosensors.[16] The detection limit ($3\sigma/K$)[17] of receptor **1** for the analysis of Cu^{2+} was calculated to be 23.5 μM (Fig. S4). The detection limit of **1** for Cu^{2+} is lower than that (31.5 μM) recommended by World Health Organization (WHO) in drinking water.[4] Therefore, **1** could be a good indicator for the detection of copper ions in drinking water.

To explore the anti-disturbance of **1** as the Cu^{2+}-selective sensor, competition experiments were performed (Fig. 3). For this purpose, **1** was treated with 12 equiv of Cu^{2+} in the presence of the same concentration of other metal ions. The absorbance at 450 nm caused by Cu^{2+} was retained with Zn^{2+}, Cd^{2+}, Mg^{2+}, Cr^{3+}, Co^{2+}, Ni^{2+}, Na^+, K^+, Ca^{2+}, Mn^{2+}, Fe^{3+} and Pb^{2+}. Instead, the absorbance of **1**-Cu^{2+} complex in the presence of Al^{3+} and Fe^{2+} was relatively low. In order to overcome the inhibitions, we have added iodide to **1**-Cu^{2+}- Al^{3+} solution and

fluoride to **1**-Cu^{2+}-Fe^{2+} one. The resulting absorbance of **1**-Cu^{2+} complex in the presence of Al^{3+} and Fe^{2+} were recovered to 89% and 84%, respectively (Fig. S5). Thus **1** can be used as a selective colorimetric sensor for Cu^{2+} detection in the presence of most competing metal ions.

To study the practical applicability, the colorimetric responses of **1** in the absence and presence of Cu^{2+} in different pH values were evaluated. As shown in Fig. 4, the receptor **1** itself was stable from pH 2 to 12. Upon the addition of Cu^{2+}, there was an apparent increase of absorbance (450 nm) at the pH range of 7 - 12. These results indicated that Cu^{2+} could be clearly detected by the naked eye or UV-vis absorption measurements using **1** over the wide pH range.

We subsequently studied the binding reversibility of Cu^{2+} to **1** in acetonitrile-water solution. Due to the high stability constant for the EDTA-Cu^{2+} complex, it was expected that EDTA would chelate Cu^{2+} from the **1**-Cu^{2+} complex, liberating **1**. As shown in Fig. 5, the absorbance of **1**-Cu^{2+} was quenched and the color changed from yellow to colorless upon the addition of 12 equiv EDTA. Introduction of an additional Cu^{2+} resulted in the recovery of absorbance and color, indicating that the binding of **1** with Cu^{2+} is chemically reversible. The absorbance (Fig. 5a) and color changes (Fig. 5b) were almost reversible even after several cycles with the sequentially alternative addition of Cu^{2+} and EDTA.

In order to study the applicability of the sensor **1** in environmental water samples, we constructed a calibration curve for the determination of Cu^{2+} by **1** (Fig. S6). It exhibited a good linear relationship between the absorbance of **1** and Cu^{2+} concentrations (0 - 10 μM) with a correlation coefficient of $R^2 = 0.9912$ (n = 3), which means that **1** could be suitable for the quantitative detection of Cu^{2+}. Then, the sensor was applied for the determination of Cu^{2+} in tap water samples. The results were summarized in Table 1, which exhibited a satisfactory recovery and R.S.D. values for the tap water samples.

To understand the sensing mechanisms of **1** toward Cu^{2+}, theoretical calculations were performed with the 1:1 stoichiometry, based on Job plot and ESI-mass spectrometry analysis. To get the energy-minimized structures of **1** and **1**-Cu^{2+} complex, the geometric optimizations were performed by DFT/B3LYP level. Especially, **1**-Cu^{2+} complex was considered by a paramagnetic character (S=1/2, DFT/uB3LYP/main group atom: 6-31G** and Cu:

Lanl2DZ/ECP). The significant structural properties of the energy-minimized structures were shown in Fig. 6. The energy minimized structure of **1** showed a V-type structure with the dihedral angle of 1N, 2N, 3C, 4O = 37.664^{o}, and the hydrogen bond was observed between 2N and 6H (Fig. 6(a)). **1**-Cu^{2+} complex exhibited a square planar structure (dihedral angle (1N, 2N, 3C, 4O) = 8.738^{o})) with the coordination of N, N and O atoms of **1** (Fig. 6(b)).

We also investigated the absorption to the singlet excited states of **1** and **1**-Cu^{2+} species via TDDFT calculations. In case of **1**, the main molecular orbital (MO) contribution of the first lowest excited state was determined for HOMO – 2 → LUMO and HOMO → LUMO + 1 transitions (341.34 nm, Fig. S7), which indicated ICT bands. **1**-Cu^{2+} complex showed that the excited states of 4th, 9th and 12th (497.47, 403.68 and 377.69 nm) were relevant to the color change (colorless to yellow) with predominant ICT and LMCT characters (Figs. S8, S9 and S10). Thus, the chelation of Cu^{2+} with **1** mainly showed the ICT and LMCT, which induced the different color change of **1** in the presence of Cu^{2+}.

Colorimetric signaling of 1 to F^-

The colorimetric sensing properties of **1** were also investigated towards various anions (CN^-, OAc^-, F^-, Cl^-, Br^-, I^-, $H_2PO_4^-$, BzO^-, N_3^- and SCN^-) in DMSO as shown in Fig. 7. Upon the addition of 30 equiv of various anions to **1**, there was no significant UV-vis spectral change in the nature of spectra except for F^- (Fig. 7a). In the presence of F^-, the receptor **1** showed a distinct spectral change and a color change from colorless to orange with an immediate response time, which was sufficiently distinct to be discriminated from other anions through naked-eye (Fig. 7b).

The interaction of receptor **1** with F^- was studied in detail by UV-vis spectroscopic titration, as shown in Fig. 8. On gradual addition of F^-, the band at 350 nm decreased, and a new band at 465 nm increased drastically. The absorbance reached a maximum at 30 equiv of fluoride with a clear isosbestic point observed at 406 nm, indicating the formation of the only one species between **1** and F^-. The color change of **1** from colorless to orange might be due to the deprotonation of phenol of **1** by F^- (Scheme 1). To further confirm the sensing mechanism between **1** and F^-, the interaction between **1** and OH^- was also investigated (Fig. S11). UV–vis

spectral change of **1** upon addition of OH^- was nearly identical to that of **1** obtained from the addition of F^-, which indicated the deprotonation between **1** and F^-. The resulting negative charge on the phenol is introduced in the receptor which causes intramolecular charge transfer (ICT) between the electron deficient -NO_2 group and the electron rich -O^- to show the UV-vis and colorimetric changes.[18]

The Job plot for the binding between **1** and F^- exhibited a 1:1 stoichiometry (Fig. S12), which was further supported by ESI-mass spectrometry analysis (Fig. S13). The negative ion mass spectrum of ESI-mass indicated that a peak at m/z = 380.67 was assignable to [**1**-H^+]$^-$ [calcd, 380.17], which is corresponding to the receptor **1**$^-$ deprotonated by fluoride. From the UV-vis titration data, the association constant for **1** with F^- was determined as 5.9×10^2 M^{-1} using the Benesi-Hildebrand equation[15] (Fig. S14). The detection limit ($3\sigma/K$)[17] of receptor **1** for the analysis of F^- was calculated to be 19.4 μM (Fig. S15).

To study the interaction between **1** and F^-, the ^1H NMR titrations of **1** were measured with different amounts of F^- (Fig. 9). In the absence of F^-, the phenolic OH proton (H_{12}) and the amine NH proton (H_8) appeared as a singlet at 13.56 and 8.25 ppm, respectively. Upon the gradual addition of F^-, the singlets of H_{12} and H_8 were broadened and finally disappeared due to hydrogen bonding with F^-. Simultaneously, the $H_{6,7}$ protons and the protons of nitropyridine moiety ($H_{9\text{-}11}$) were shifted upfield. These results suggested that the -NH and -OH protons might hydrogen bond to F^-, and eventually undergo the deprotonation (Scheme 1).

To test whether **1** can detect F^- selectively even in the presence of other anions, competitive experiment was conducted (Fig. 10). **1** was treated with 30 equiv of F^- in the presence of several anions. The results indicated that the competitive anions did not lead to any significant spectral (Fig. 10a) and color change (Fig. 10b), and that F^- ions still resulted in the similar absorbance and color in the presence of competitive anions. Thus, **1** could be used as a selective chemosensor for F^- by the colorimetric mode.

Conclusion

We synthesized a bi-functional colorimetric chemosensor based on the combination of 8-

hydroxyljulolidine-9-carboxaldehyde and *N*-(2-aminoethyl)-5-nitropyridin-2-amine. The sensor **1** exhibited a colorimetric response from colorless to yellow upon binding to Cu^{2+} in aqueous solution. The binding of the sensor **1** and Cu^{2+} was also chemically reversible with EDTA. The recovery studies of the water samples added with Cu^{2+} showed a satisfactory recovery and R.S.D. values. Additionally, the sensing mechanism of **1** toward Cu^{2+} was explained by theoretical calculations. Furthermore, **1** can selectively detect F^- among the various anions with the colorimetric change from colorless to orange. In particular, **1** can distinguish F^- in the presence of other anions such as CH_3COO^- and CN^-. These results demonstrated that chemosensor **1** will be useful for development of new chemosensor for recognizing both cations and anions.

Experimental

Materials and equipment

All the solvents and reagents (analytical and spectroscopic grade) were purchased from Sigma-Aldrich. ^1H and ^{13}C NMR spectra were recorded on a Varian 400 MHz and 100 MHz spectrometer and chemical shifts were recorded in ppm. Electro spray ionization mass spectra (ESI-MS) were collected on a Thermo Finnigan (San Jose, CA, USA) LCQ_{TM} Advantage MAX quadrupole ion trap instrument by infusing samples directly into the source using a manual method. Spray voltage was set at 4.2 kV, and the capillary temperature was at 80 ^oC. Absorption spectra were recorded at room temperature using a Perkin Elmer model Lambda 25 UV/Vis spectrometer. Elemental analysis for carbon, nitrogen and hydrogen was carried out using a Flash EA 1112 elemental analyzer (thermo) at the Organic Chemistry Research Center of Sogang University, Korea.

Synthesis of receptor 1

An ethanolic solution of 8-hydroxyjulolidine-9-carboxaldehyde (0.23 g, 1 mmol) was added to *N*-(2-aminoethyl)-5-nitropyridine-2-amine (0.22 g, 1.2 mmol) in ethanol (10 mL). The reaction solution was stirred for 2 d at room temperature. The yellow powder was filtered and washed with ethanol and diethyl ether. The yield: 0.32 g (84 %); ^1H NMR (400 MHz DMSO-d_6, ppm):

δ 13.54 (s, 1H), 8.90 (s, 1H), 8.22 (s, 1H), 8.09 (s, 1H), 8.08 (s, 1H), 6.64 (s, 1H), 6.60 (d, *J* = 8 MHz, 1H), 3.64 (s, 4H), 3.17 (m, *J* = 6 MHz, 4H), 2.58 (t, *J* = 6 MHz), 1.84 (m, *J* = 6 MHz, 4H); ^{13}C NMR (100 MHz DMSO-d_6, ppm): 165.14, 161.48, 159.33, 146.79, 145.84, 134.26, 131.79, 128.83, 111.54, 108.60, 107.29, 105.59, 56.03, 49.29, 48.91, 42.00, 26.61, 21.60, 20.68, 20.07. ESI-MS m/z (M + H^+): calcd, 382.19; found, 382.33. Anal. Calc. for $C_{20}H_{23}N_5O_3$: C, 62.98; H, 6.08; N, 18.36. Found: C, 63.21; H, 5.93; N, 18.27 %.

UV-vis titration

For Cu^{2+}, the UV-vis titration experiment of **1** was carried out by adding aliquots of 3-39 μL of $Cu(NO_3)_2{\cdot}2.5H_2O$ solution (20 mM) to 3 mL of **1** solution (20 μM, 7:3, acetonitrile/bis-tris buffer v/v; 10 mM bis-tris, pH 7.0). The spectra were recorded a minute after the solution was completely mixed.

For F^-, the UV-vis titration experiment of **1** was carried out by adding aliquots of 6-60 μL of tetraethyl ammonium fluoride (TEAF) solution (100 mM) to 3 mL of **1** solution (20 μM in DMSO). The spectra were recorded a minute after the solution was completely mixed.

Job plot measurements

For Cu^{2+}, stock solution of receptor **1** (10 mM) was prepared in 1 mL of acetonitrile/bis-tris buffer (7:3; v/v). Cu^{2+} solution (10 mM) was prepared by dissolving nitrate salts in acetonitrile/bis-tris buffer (7:3; v/v, 1 mL). 30, 27, 24, 21, 18, 15, 12, 9, 6 and 3 μL of the **1** solution were taken and transferred to vials. Each vial was diluted with acetonitrile/bis-tris buffer (7:3; v/v) to make a total volume of 2.97 mL. Then, 0, 3, 6, 9, 12, 15, 18, 21, 24, 27 and 30 μL of the Cu^{2+} solution were added to each diluted **1** solution. Each vial had a total volume of 3 mL. After shaking the vials for a minute, UV-vis spectra were taken at room temperature.

For F^-, stock solution of receptor **1** (10 mM) was prepared in 1 mL of DMSO. F^- solution (10 mM) was prepared by dissolving TEAF salt in DMSO (1 mL). 15, 13.5, 12, 10.5, 9, 7.5, 6, 4.5, 3 and 1.5 μL of the **1** solution were taken and transferred to vials. Each vial was diluted with DMSO to make a total volume of 2.985 mL. Then, 0, 1.5, 3, 4.5, 6, 7.5, 9, 10.5, 12, 13.5 and 15 μL of the F^- solution were added to each diluted **1** solution. Each vial had a total volume of 3 mL. After shaking the vials for a minute, UV-vis spectra were taken at room

temperature.

Competition experiments

For Cu^{2+}, stock solution of receptor **1** (5 mM) was prepared in 1 mL of acetonitrile/bis-tris buffer (7:3; v/v). Solution samples (20 mM) of metal ions were prepared by dissolving the corresponding salts in a mixture of acetonitrile/bis-tris buffer (7:3; v/v, 1 mL). 36 μL aliquot of each metal-ion stock solution and 36 μL of Cu^{2+} solution were diluted into a 3 mL of mixture of acetonitrile/bis-tris buffer (7:3; v/v). Then, 12 μL of the **1** solution was added into the mixed solution to make 20 μM. After shaking the vials for a minute, UV-vis spectra were taken at room temperature.

For F^-, stock solution of receptor **1** (5 mM) was prepared in 1 mL of DMSO. Solution samples (20 mM) of anions were prepared by dissolving the corresponding salts in DMSO (1 mL). 48 μL aliquot of each anion stock solution and 48 μL of F^- solution were diluted into a 3 mL of DMSO. Then, 12 μL of the **1** solution was added into the mixed solution to make 20 μM. After shaking the vials for a minute, UV-vis spectra were taken at room temperature.

Theoretical calculation methods of 1 with Cu^{2+}

All DFT/TDDFT calculations based on the hybrid exchange-correlation functional B3LYP[19] were carried out using Gaussian 03 program[20]. The 6-31G** basis set[21] was used for the main group elements, whereas the Lanl2DZ effective core potential (ECP)[22] was employed for Cu. In vibrational frequency calculations, there was no imaginary frequency for the optimized geometries of **1** and **1**-Cu^{2+} complex, suggesting that these geometries represented local minima. For all calculations, the solvent effect of water was considered by using the Cossi and Barone's CPCM (conductor-like polarizable continuum model).[23] To investigate the electronic properties of singlet excited states, time-dependent DFT (TDDFT) was performed in the ground state geometries of **1** and **1**-Cu^{2+}. The 35 singlet-singlet excitations were calculated and analyzed. The GaussSum 2.1[24] was used to calculate the contributions of molecular orbitals in electronic transitions.

^{1}H NMR titration of 1 with F^-

For ^{1}H NMR titration of receptor **1** with F^-, four NMR tubes of receptor **1** (3.81 mg, 0.01 mmol) dissolved in DMSO-d_6 (700 μL) were prepared and then four different concentrations (0, 0.005, 0.01 and 0.02 mmol) of TEAF dissolved in DMSO-d_6 were added to each solution of receptor **1**. After shaking them for a minute, ^{1}H NMR spectra were obtained at room temperature.

Acknowledgements

Basic Science Research Program through the National Research Foundation of Korea (NRF) funded by the Ministry of Education, Science and Technology (NRF-2014R1A2A1A11051794 and NRF-2015R1A2A2A09001301) is gratefully acknowledged. We thank Nano-Inorganic Laboratory, Department of Nano & Bio Chemistry, Kookmin University to access the Gaussian 03 program packages.

Supplementary information

Supplementary material associated with this article can be found, in the online version.

References

1 (*a*) M. Kumar, N. Kumar and V. Bhalla, *Dalton Trans.*, 2012, **41**, 10189-10193; (*b*) D. Karak, S. Lohar, A. Banerjee, A. Sahana, I. Hauli, S. K. Mukhopadhyay, J. S. Matalobos and D. Das, *RSC Adv.*, 2012, **2**, 12447-12454; (*c*) Y. Peng, Y.-M. Dong, M. Dong and Y.-M. Wang, *J. Org. Chem.*, 2012, **77**, 9072-9080; (*d*) X. Chen, S. Nam, G. Kim, N. Song, Y. Jeong, I. Shin, S. K. Kim, J. Kim, S. Park and J. Yoon, *Chem. Commun.*, 2010, **46**, 8953-8955; (*e*) S. Devaraj, V. S. Elanchezhian and M. Kandaswamy, *Inorg. Chem. Commun.*, 2011, **14**, 1596-1601.

2 (*a*) E. Gaggelli, H. Kozlowski, D. Valensin and G. Valensin, *Chem. Rev.*, 2006, **106**, 1995-2044; (*b*) I. A. Koval, P. Gamez, C. Belle, K. Selmeczi and J. Reedijk, *Chem. Soc. Rev.*, 2006, **35**, 814-840; (*c*) D. Maiti, H. R. Lucas, A. A. N. Sarjeant and K. D. Karlin, *J. Am. Chem. Soc.*, 2007, **129**, 6998-6999; (*d*) Y. J. Na, Y. W. Choi, J. Y. Yun, K.-M. Park, P.-S. Chang and C. Kim, *Spectrochim. Acta, Part A* , 2015, **136**, 1649-165

3 (*a*) R. Krämer, *Angew. Chem. Int. Ed.*, 1998, **37**, 723-772; (*b*) Y. K. Jang, U. C. Nam, H. L. Kwon, I. H. Hwang and C. Kim, *Dyes Pigm.*, 2013, **99**, 6-13; (*c*) J. Y. Noh, G. J. Park, Y. J. Na, H. Y. Jo, S. A. Lee and C. Kim, *Dalton Trans.*, 2014, **43**, 5652-5656; (*d*) H. Kim, Y. J. Na, E. J. Song, K. B. Kim, J. M. Bae and C. Kim, *RSC Adv.*, 2014, **4**, 22463-22469; (*e*) S. Wu, T. Wang and S. Liu, *Tetrahedron*, 2010, **66**, 9655-9658; (*f*) J. Yeh, W. Chen, S. Liu and S. Wu, *New J. Chem.*, 2014, **38**, 4434-4439; (*g*) H. Yang, H. Song, Y. Zhu and S. Yang, *Tetrahedron Lett.*, 2012, **53**, 2026-2029.

4 WHO. WHO guidelines values for chemicals that are of health significance in drinking water, Guidelines for Drinking Water Quality, Geneva, 3rd edn, 2008.

5 (*a*) J. H. Kim, J. Vicens and J. S. Kim, *Tetrahedron Lett.*, 2009, **50**, 983-987; (*b*) J. Shao, H. Lin and H. K. Lin, *Talanta*, 2008, **77**, 273-277; (*c*) D. A. Jose, D. K. Kumar, B. Ganguly and A. Das, *Org. Lett.*, 2004, **6**, 3445-3448; (*d*) R. G. Schamschula, *Annu. Rev. Nutr.*, 1981, **1**, 427-435; (*e*) H. S. Horowitz, *J. Public. Health Dent.*, 2003, **63**, 3-81; (*f*) M. Kleerekoper, *Endocrinol. Metab. Clin. North Am.*, 1998, **27**, 441; (*g*) G. J. Park, H. Y. Jo, K. Y. Ryu and C. Kim, *RSC. Adv.*, 2014, **4**, 63882-63890.

6 (*a*) Y. Kim and F. P. Gabba¨ı, *J. Am. Chem. Soc.*, 2009, **131**, 3363-3369; (*b*) K. Tayade, S. K. Sahoo, A. Singh, N. Singh, P. Mahulikar, S. Attarde and A. Kuwar, *Sens. Actuators, B*, 2014, **202**, 1333-1337; (*c*) A. Bamesberger, C. Schwartz, Q. Song, W. Han, Z. Wang and H. Cao, *New J. Chem.*, 2014, **38**, 884-888; (*d*) P. G. Sutariya, N. R. Modi, A. Pandya, B. K. Joshi, K. V. Joshia and S. K. Menon, *Analyst*, 2012, **137**, 5491-5494; (*e*) L. Zang, D. Wei, S. Wang and S. Jiang, *Tetrahedron*, 2012, **68**, 636-641; (*f*) S. Sharma, M. S. Hundal and G. Hundal, *Tetrahedron Lett.*, 2013, **54**, 2423-2427.

7 (*a*) B. Moss, Chem. Ind., 1996, **11**, 407-411; (*b*) J. M. Tomich, D. Wallace, K. Henderson, K. E. Mitchell, G. Radke, R. Brandt, C. Ambler, A. J. Scott, J. Grantham, L. Sullivan and T. Iwamoto, *Biophys. J.*, 1998, **74**, 256-267; (*c*) S. Matsuo, K. Kiyomiya and M. Kurebe, *Arch. Toxicol.*, 1998, **72**, 798-806; (*d*) D. Briancon, *Rev. Rhum.*, 1997, **64**, 78-81.

8 T. G. Jo, Y. J. Na, J. J. Lee, M. M. Lee, S. Y. Lee and C. Kim, *New. J. Chem.*, 2015, **39**, 2580-2587.

9 (*a*) V. A. Fassel, *Science*, 1978, **202**, 183-191; (*b*) W. Yang, D. Jaramillo, J. J. Gooding, D. B. Hibbert, R. Zhang, G. D. Willet and K. J. Fishera, *Chem. Commun.*, 2001, **19**, 1982-1983; (*c*) A. P. S. Gonsales, M. A. Firmino, C. S. Nomura, F. R. P. Rocha, P. V. Olivera and I. Gaubeur, *Anal. Chim. Acta*, 2009, **636**, 198-204; (*d*) J. S. Becker, A. Matusch, C. Depboylu, J. Dobrowolska and M. V. Zoriy, *Anal. Chem.*, 2007, **79**, 6074-6080.

10 (*a*) J. Xu, K. Liu, D. Di, S. Shao and Y. Guo, *Inorg. Chem. Commun.*, 2007, **10**, 681-684; (*b*) C. Suksai and T. Tuntulani, *Chem. Soc. Rev.*, 2003, **32**, 192-202; (*c*) C. Liu, J. Xu, F. Yang, W. Zhou, Z. Li, L. Wei and M. Yu, *Sens. Actuators, B*, 2015, **212**, 364-370.

11 (*a*) N. Narayanaswamy and T. Govindaraju, *Sens. Actuators, B*, 2012, **161**, 304-310; (*b*) D. Maity, A. K. Manna, D. Karthigeyan, T. K. Kundu, S. K. Pati and T. Govindaraju, *Chem. Eur. J.*, 2011, **17**, 11152-11161; (*c*) Y. J. Na, I. H. Hwang, H. Y. Jo, S. A. Lee, G. J. Park and C. Kim, *Inorg. Chem. Commun.*, 2013, **35**, 342-345; (*d*) J. Y. Noh, S. Kim, I. H. Hwang, G. Y. Lee, J. Kang, S. H. Kim, J. Min, S. Park and C. Kim, *Dyes Pigm.*, 2013, **99**, 1016-1021.

12 M. Iniya, D. Jeyanthi, K. Krishnaveni and D. Chellappa, *J. Lumin.*, 2015, **157**, 383-389.

13 (*a*) E. J. Song, J. Kang, G. R. You, G. J. Park, Y. Kim, S. J. Kim, C. Kim and R. G. Harrison, *Dalton Trans.*, 2013, **42**, 15514-15520; (*b*) G. R. You, G. J. Park, J. J. Lee and C. Kim, *Dalton Trans.*, 2015, **44**, 9120-9129.

14 S. S. Qian, X. S. Cheng, Z. L. You and H. L. Zhu, *Russ. J. Coord. Chem.*, 2013, **39**, 704-709.

15 H. A. Benesi and J. H. Hildebrand, *J. Am. Chem. Soc.*, 1949, **71**, 2703-2707.

16 (*a*) F. Yu, W. Zhang, P. Li, Y. Xing, L. Tong, J. Ma and B. Tang, *Analyst*, 2009, **134**, 1826-1833; (*b*) Y. Xiang, A. Tong, P. Jin and Y. Ju, *Org. Lett.*, 2006, **8**, 2863-2866; (*c*) S. Wu, K. Du and Y. Sung, *Dalton Trans.*, 2010, **39**, 4363-4368; (*d*) G. H. Wu, D. X. Wang, D. Y. Wu, Y. Gao and Z. Q. Wang, *J. Chem. Sci.*, 2009, **121**, 543-548; (*e*) D. Udhayakumari, S. Velmathi, W. -C. Chen and S. -P. Wu, *Sens. Actuators B*, 2014, **204**, 375-381; (f) G. Li, F. Tao, H. Wang, Y. Li and L. Wang, *Sens. Actuators B*, 2015, **211**, 325-331; (g) G. Li, F. Tao, H. Wang, L. Wang, J. Zhang, P. Ge, L. Liu, T. Tong and S. Sun, *RSC Adv.*, 2015, **5**, 18983-18989; (h) L. Liu, A. Wang, G. Wang, J. Li and Y. Zhou, *Sens. Actuators B*, 2015, **215**, 388-395; (i) S. Hu, J. Song, F. Zhao, X. Meng and G. Wu, *Sens. Actuators B*, 2015, **215**, 241-248; (j) J. J. Lee, Y. W. Choi, G. R. You, S. Y. Lee and C. Kim, *Dalton Trans.*, 2015, **44**, 13305-13314.

17 Y. K. Tsui, S. Devaraj and Y. P. Yen, *Sens. Actuators, B*, 2012, **161**, 510-519.

18 (*a*) M. A. Kaloo and J. Sankar, *Analyst*, 2013, **138**, 4760-4763; (*b*) R. Sheng, P. Wang, Y. Gao, Y. Wu, W. Liu, J. Ma, H. Li and S. Wu, *Org. Lett.*, 2008, **10**, 5015-5018; (*c*) Y. Jiang, H. Zhao, Y.Q. Lin, N. N. Zhu, Y. R. Ma and L. Q. Mao, *Angew. Chem. Int. Ed.*, 2010, **122**, 4910-4914; (*e*) S. Devaraj, D. Saravanakumar and M. Kandaswamy, *Sens. Actuators, B*, 2009, **136**, 13-19.

19 (*a*) A. D. Becke, *J. Chem. Phys.*, 1993, **98**, 5648-5652; (*b*) C. Lee, W. Yang and R. G. Parr, *Phys. Rev. B*, 1988, **37**, 785-789.

20 M. J. Frisch, G. W. Trucks, H. B. Schlegel, G. E. Scuseria, M. A. Robb, J. R. Cheeseman, J. A. Montgomery, Jr., T. Vreven, K. N. Kudin, J. C. Burant, J. M. Millam, S. S. Iyengar, J. Tomasi, V. Barone, B. Mennucci, M. Cossi, G. Scalmani, N. Rega, G. A. Petersson, H.

Nakatsuji, M. Hada, M. Ehara, K. Toyota, R. Fukuda, J. Hasegawa, M. Ishida, T. Nakajima, Y. Honda, O. Kitao, H. Nakai, M. Klene, X. Li, J. E. Knox, H. P. Hratchian, J. B. Cross, V. Bakken, C. Adamo, J. Jaramillo, R. Gomperts, R. E. Stratmann, O. Yazyev, A. J. Austin, R. Cammi, C. Pomelli, J. W. Ochterski, P. Y. Ayala, K. Morokuma, G.A. Voth, P. Salvador, J. J. Dannenberg, V. G. Zakrzewski, S. Dapprich, A. D. Daniels, M.C. Strain, O. Farkas, D. K. Malick, A. D. Rabuck, K. Raghavachari, J. B. Foresman, J. V. Ortiz, Q. Cui, A. G. Baboul, S. Clifford, J. Cioslowski, B. B. Stefanov, G. Liu, A. Liashenko, P. Piskorz, I. Komaromi, R. L. Martin, D. J. Fox, T. Keith, M. A. Al-Laham, C. Y. Peng, A. Nanayakkara, M. Challacombe, P. M. W. Gill, B. Johnson, W. Chen, M. W. Wong, C. Gonzalez, and J. A. Pople, Gaussian 03, Revision D.01, Gaussian, Inc., Wallingford CT, 2004.

21 (*a*) P. J. Hay and W. R. Wadt, *J. Chem. Phys.*, 1985, **82**, 270-283; (*b*) P. J. Hay and W. R. Wadt, *J. Chem. Phys.*, 1985, **82**, 284-298.

22 P. J. Hay and W. R. Wadt, *J. Chem. Phys.*, 1985, **82**, 299-310.

23 (*a*) V. Barone and M. Cossi, *J. Phys. Chem. A*, 1998, **102**, 1995-2001; (*b*) M. Cossi and V. Barone, *J. Chem. Phys.*, 2001, **115**, 4708-4717.

24 M. M. O'Boyle, A. L. Tenderholt and K. M. Langner, *J. Comput. Chem.*, 2008, **29**, 839-845.

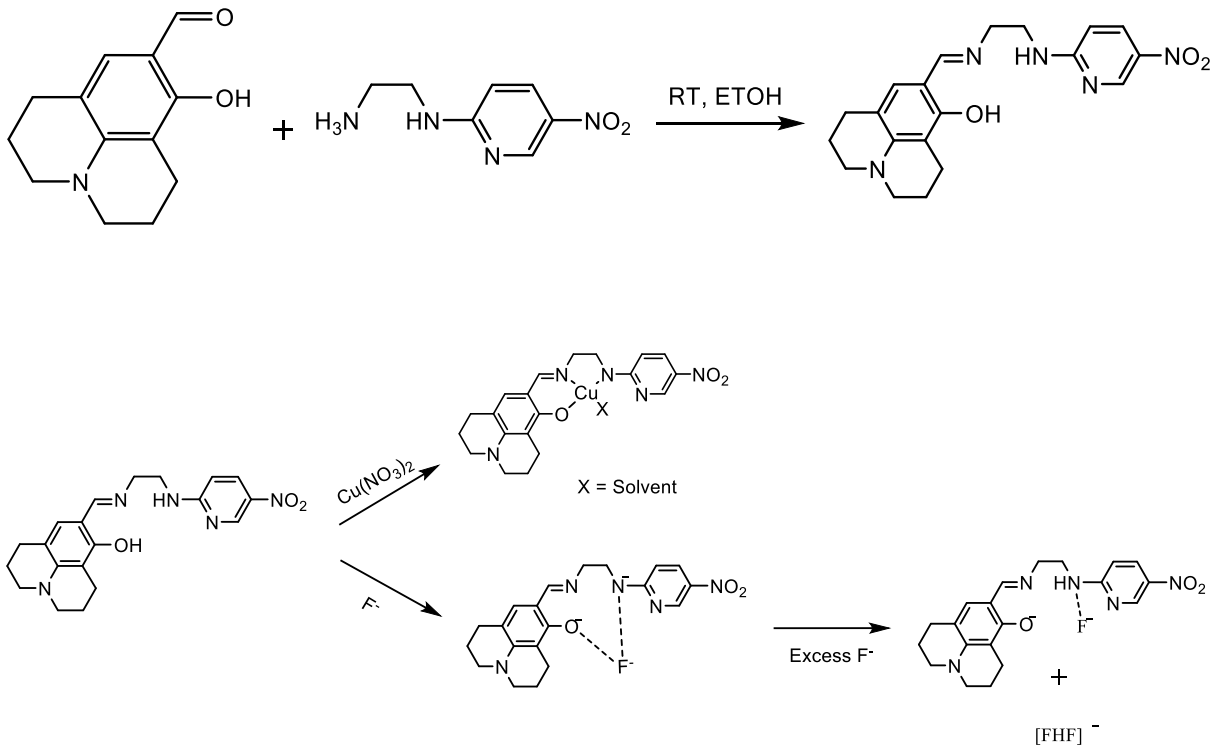

Scheme 1. Synthesis of **1** and sensing mechanisms of Cu^{2+} and F^- by **1**.

Table 1. Determination of Cu(II) in water samples.

Sample	Cu(II) added (μmol/L)	Cu(II) found (μmol/L)	Recovery (%)	R.S.D (n=3) (%)
Tap water	0.00	0.23		0.06
	6.00	6.24	100.2	0.01

Conditions: [**1**] = 10 μmol/L, water/acetonitrile (3 : 7, v/v) at pH 7.0 buffered by 10 mmol/L bis-tris.

Figure captions

Fig. 1 (a) UV-vis spectral changes of **1** (20 μM) upon addition of 12 equiv of various metal ions in acetonitrile-water (7:3, v/v). (b) Colorimetric changes of **1** (20 μM) upon the addition of various metal ions (12 equiv).

Fig. 2 Absorption spectral changes of **1** (20 μM) after addition of increasing amounts of Cu^{2+} in acetonitrile-water (7:3, v/v). Inset: Absorption at 450 nm versus the number of equiv of Cu^{2+} added.

Fig. 3 (a) Competitive selectivity of **1** (20 μM) toward Cu^{2+} (12 equiv) in the presence of other metal ions (12 equiv) in acetonitrile-water (7:3, v/v). (b) Colorimetric changes of **1** (20 μM) in the presence of Cu^{2+} (12 equiv) and other metal ions (12 equiv).

Fig. 4 Absorbance of **1** upon addition of 12 equiv of Cu^{2+} at various range of pH.

Fig. 5 (a) Absorbance of **1** (20 μM) after the sequential addition of Cu^{2+} and EDTA. (b) The color changes of **1** (20 μM) after the sequential addition of Cu^{2+} and EDTA.

Fig. 6 The energy-minimized structures of (a) **1** and (b) **1**-Cu^{2+} complex.

Fig. 7 (a) UV-vis spectral changes of **1** (20 μM) upon addition of 30 equiv of various anions in DMSO. (b) Colorimetric changes of **1** (20 μM) upon the addition of various anions (30 equiv).

Fig. 8 Absorption spectral changes of **1** (20 μM) after addition of increasing amounts of F^- in DMSO. Inset: Absorption at 465 nm versus the number of equiv of F^- added.

Fig. 9 ^1H NMR titration of **1** with F^-.

Fig. 10 (a) Competitive selectivity of **1** (20 μM) toward F^- (30 equiv) in the presence of other anions (30 equiv) in DMSO. (b) Colorimetric changes of **1** (20 μM) in the presence of F^- (30 equiv) and other anions (30 equiv).

(a)

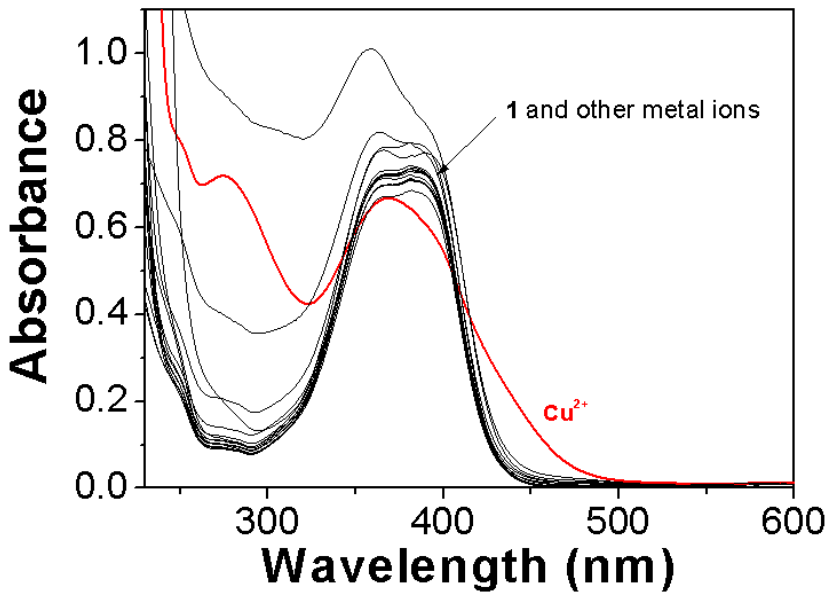

(b)

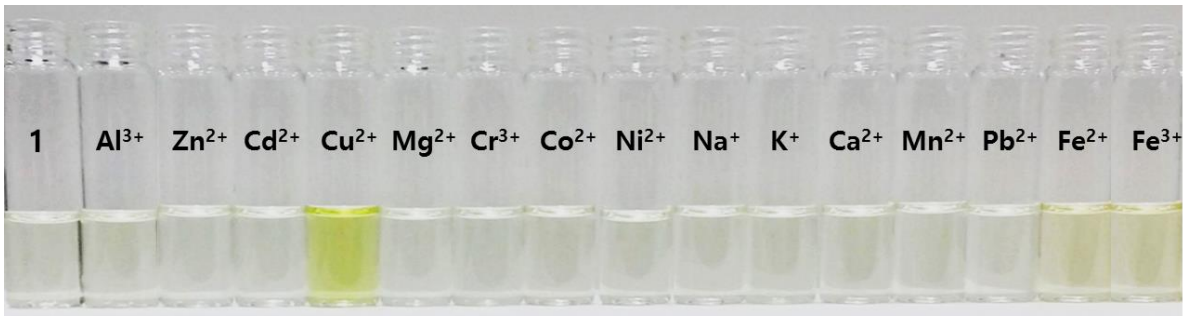

Fig. 1

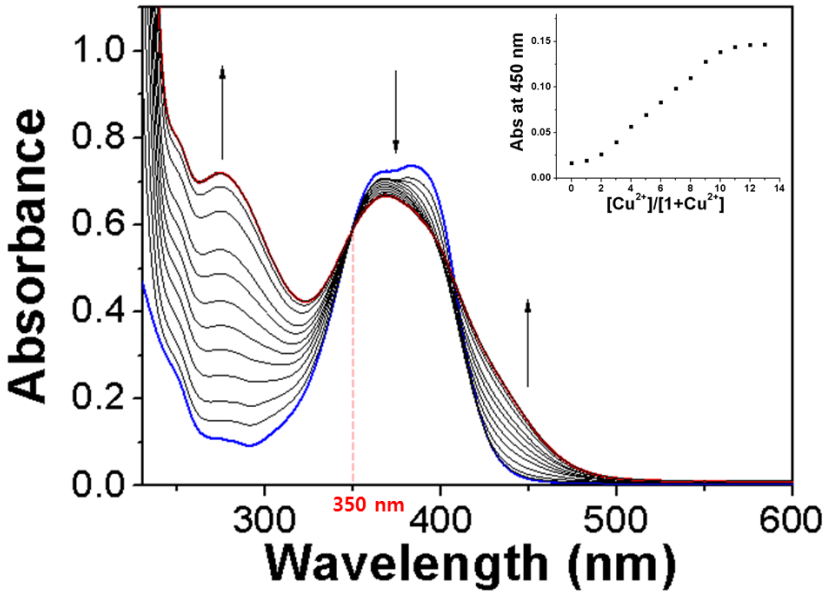

Fig. 2

(a)

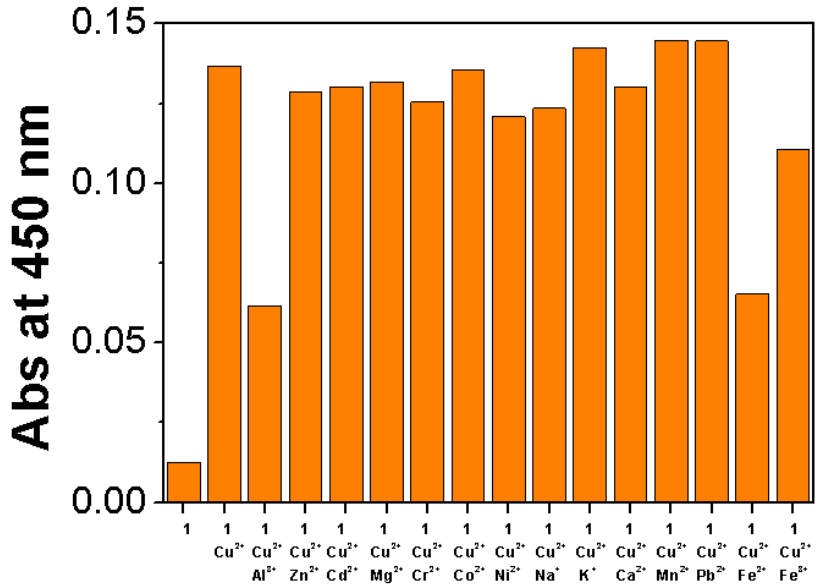

(b)

Fig. 3

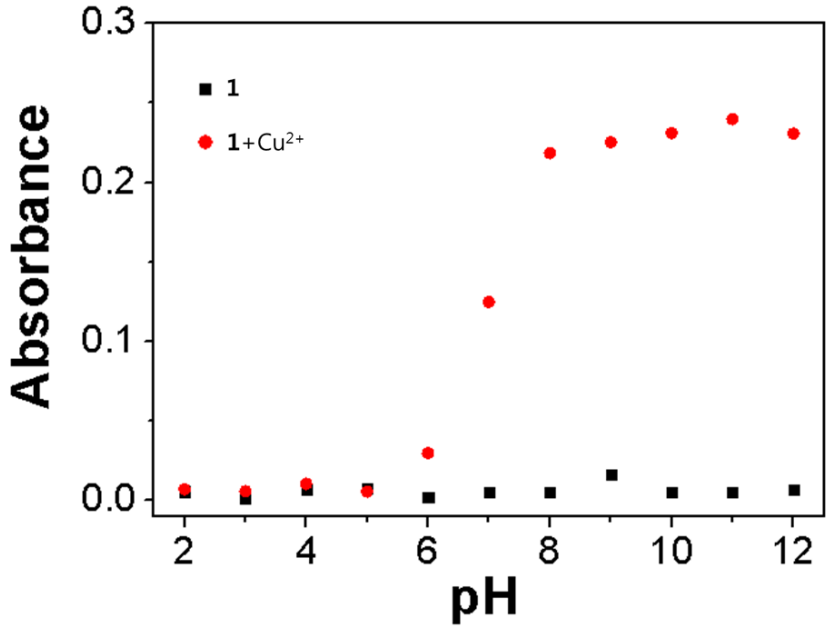

Fig. 4

(a)

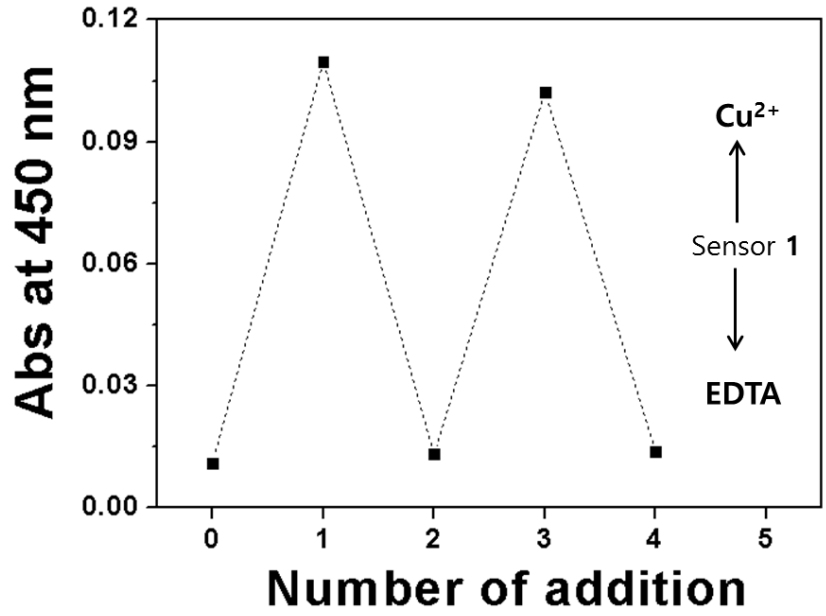

(b)

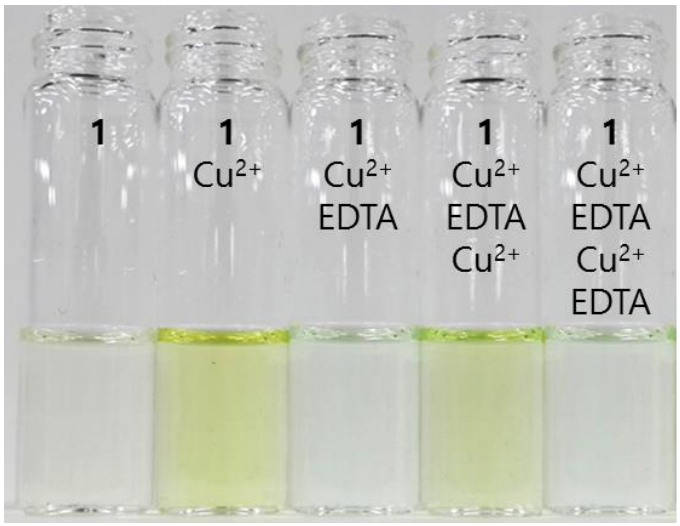

Fig. 5

(a)

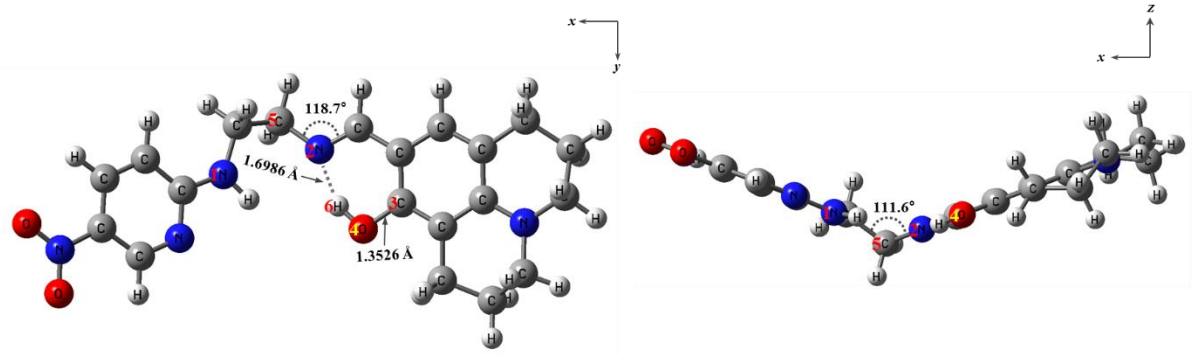

Dihedral angle (1N, 2N, 3C, 4O) : 37.664°

(b)

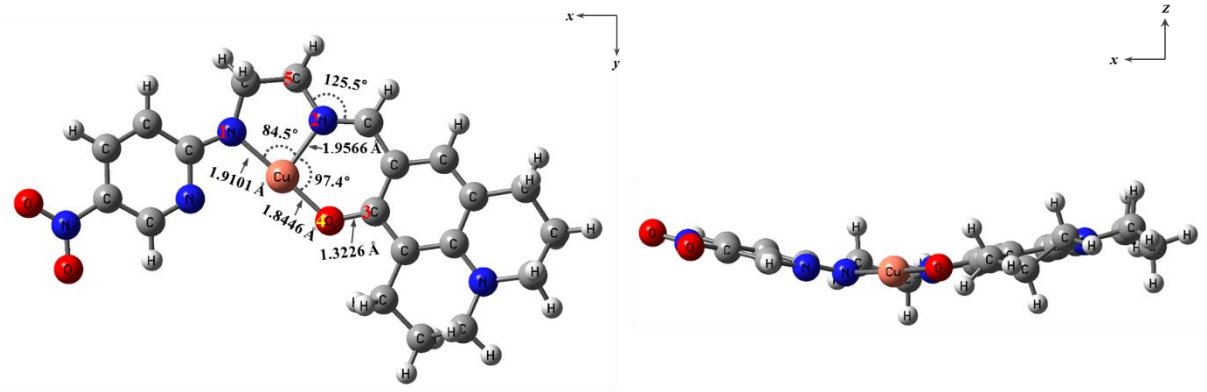

Dihedral angle (1N, 2N, 3C, 4O) : 8.738

Fig. 6

(a)

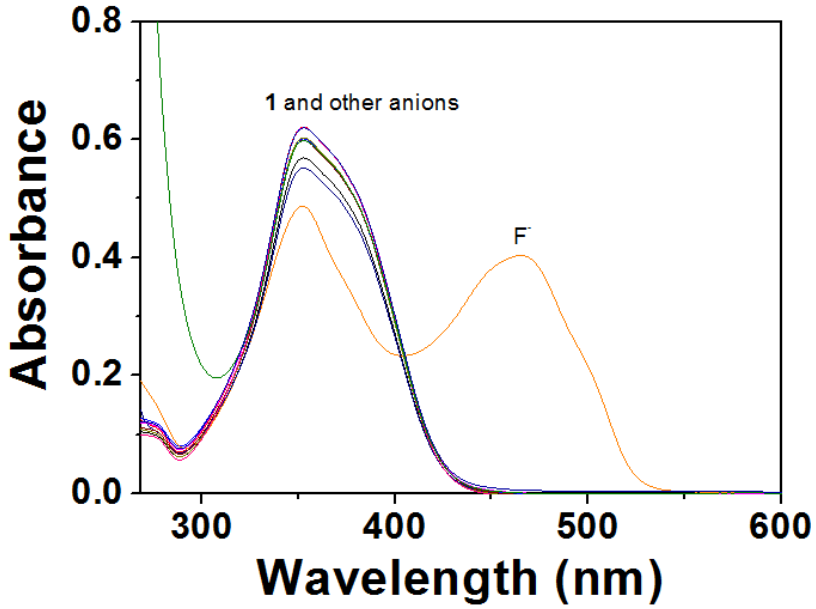

(b)

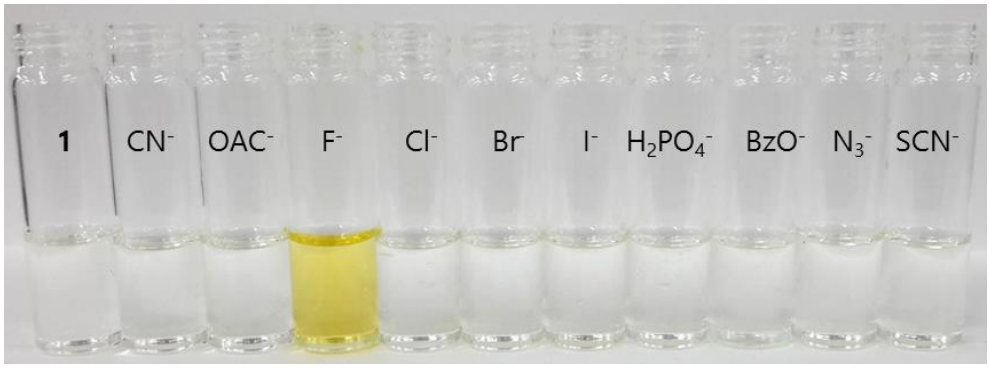

Fig. 7

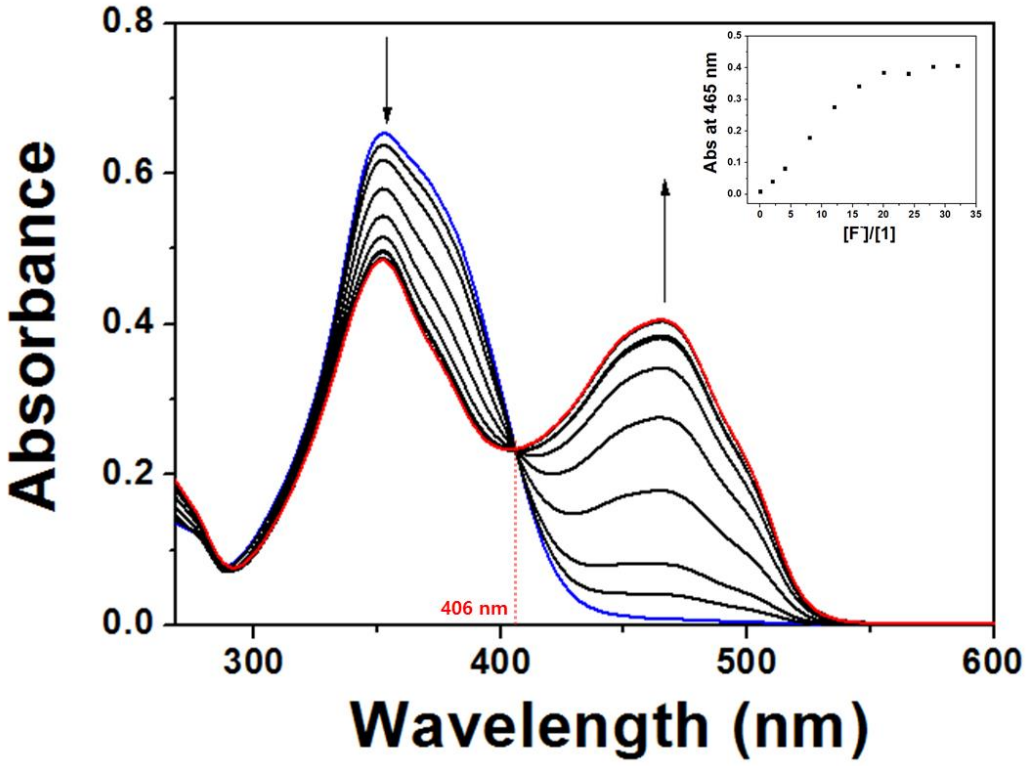

Fig. 8

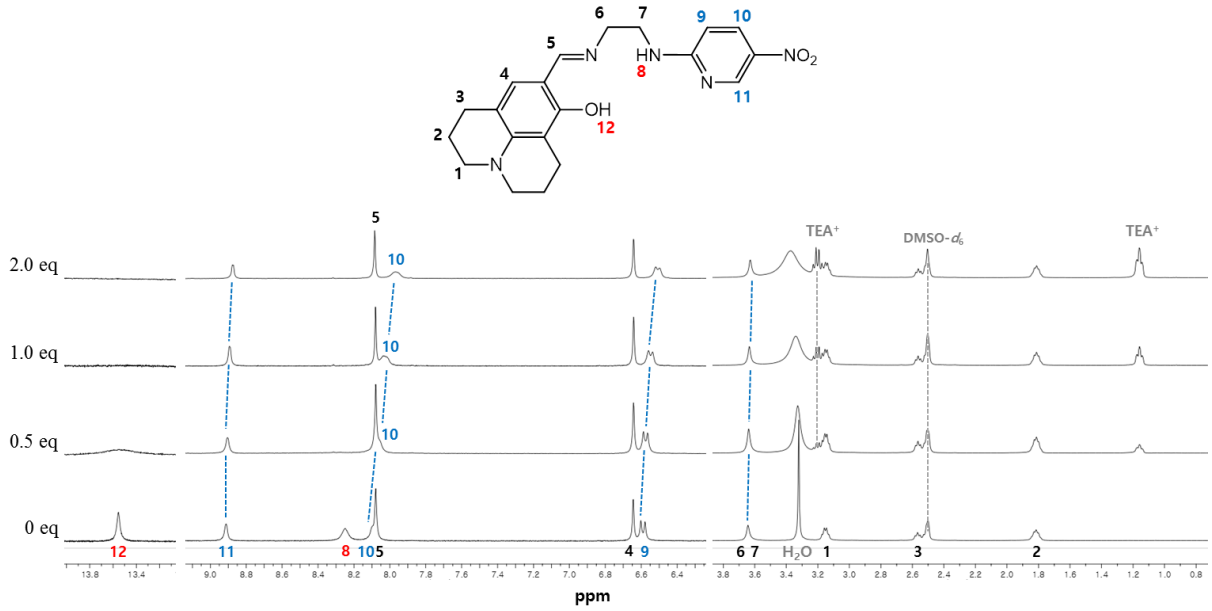

Fig. 9

(a)

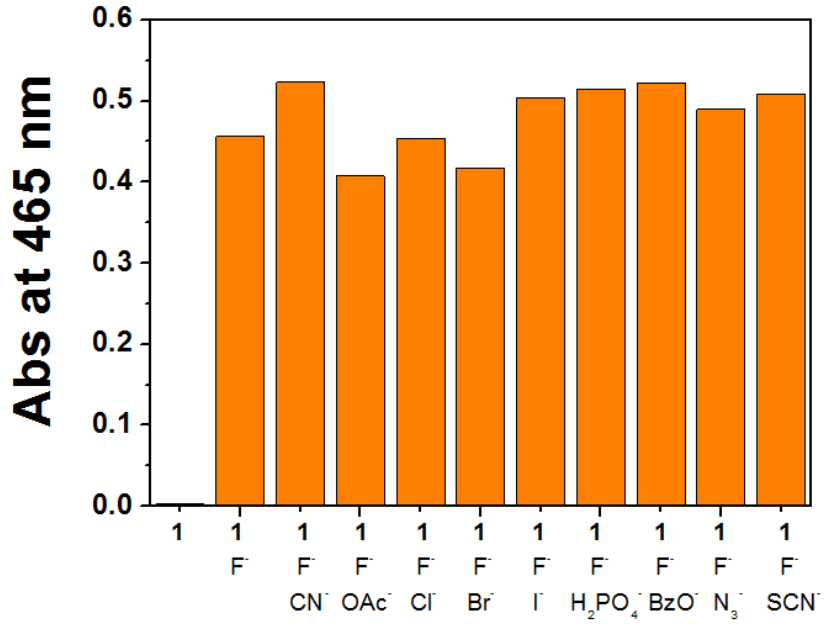

(b)

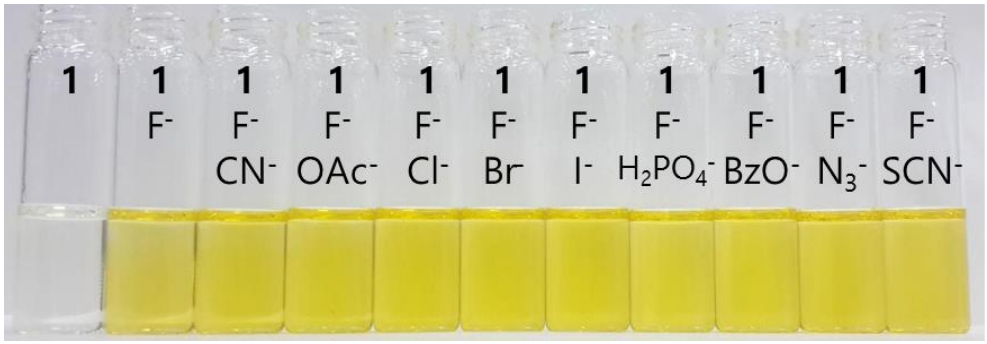

Fig. 10